Core Cross-Linked Nanoparticles from Self-assembling PolyFMA-Based Micelles. Encapsulation of Lipophilic Molecules

Elsa Galbis [a], M.-Violante de-Paz [a,], Nieves Iglesias [a], Bertrand Lacroix [b], Ana Alcudia [a], Juan A. Galbis[a]*

[a]. Dpto. Química Orgánica y Farmacéutica, Facultad de Farmacia, Universidad de Sevilla, 41012-Seville, Spain.
[b]. Instituto de Ciencia de Materiales de Sevilla, CSIC - Universidad de Sevilla, Av. Américo Vespucio 49, 41092 Seville, Spain.

* E-mail: vdepaz@us.es

Abstract

The present work describes the preparation of stable organic nanoparticles with potential use as "smart" drug delivery systems capable of encapsulating lipophilic molecules to exert their therapeutic action under the appropriate stimulus. A well-defined self-assembly hydrophilic-hydrophobic di-block copolymer has been synthesized via atom transfer radical polymerization (ATRP). The hydrophilic block is based on a random copolymer with DMA and HEMA units, while the hydrophobic component is a linear random copolymer of DEA and FMA. Stabilization of the nanoparticles by means of core cross-linking is addressed by Diels-Alder reactions between the furan rings of the hydrophobic blocks and the synthesized bisdienophiles; the influence of both the cross-linking agent and the degree of cross-linking in the process is discussed. The incorporation of a therapeutic agent (pilocarpine) and a lipophilic fluorescent molecule (pyrene) is evaluated. When pyrene was immersed into the micelles, there was a significant boost of the fluorescence emission (from 10- to 40-fold), due to the hydrophobic environment of the inner part of the nanoparticles. Pilocarpine is also able to be encapsulated by the prepared systems. Drug release is triggered by a reduction in the pH of the media and is strongly dependent on the degree of cross-linking achieved.

Keywords: stimulus-response nanoparticles, core cross-linking, drug loading, Diels-Alder reaction, pilocarpine

1. Introduction

A number of diseases are currently a threat to the health of the population and, in parallel, a bunch of different therapeutic strategies have come into play to combat them. As on numerous occasions, nature has inspired the design of therapeutic alternatives, such as the ability to respond to a stimulus, which is a basic process of living systems. In line with this, materials that respond to external stimuli—*i.e.*, changes in temperature, pH, light, or electric field, the presence or absence of certain chemical products, and ionic strength—have been synthesized. The fascinating "stimulus-response" behavior of these "smart" polymers has sparked off the development of new applications in diverse fields such as biomedicine, paints, tissue engineering, sensors, and more [1–4].

Since the mid-90s, techniques of living polymerizations have been extensively developed, including oxyanionic polymerizations [5], atom transfer radical polymerizations (ATRP) [6,7], and radical addition-fragmentation chain-transfer polymerizations (RAFT) [8]. All those techniques lead to the production of polymers with low polydispersities and well-controlled compositions and molecular weights from a wide variety of monomers, in contrast to classical radical polymerization.

The so-called amphiphilic block-copolymers constitute a specific type of copolymers of special interest because of their potential ability to self-assemble into nanoparticles (NPs). Thus, when these copolymers are dissolved in a solvent that is thermodynamically good for one block but poor for the other, the latter is embedded in a separate phase, leading to structures with possible applications in paints, cosmetics, drug delivery, electrical and electro-optical materials, metallic nanoclusters, biosensors, gene therapy, and more [9].

The administration of lipophilic drugs is associated with a number of drawbacks depending on the route of administration [10], besides some inherent disadvantages, such as the need for

reiterative dose administration at certain intervals; and monitoring drug concentrations so that they are within the therapeutic range (ratio between the dose of a drug that produces a targeted therapeutic effect and that capable of causing a toxic effect); a further challenge is the administration of drugs with a marked variability in their kinetic behavior. Hence, new methods for the administration of lipophilic drugs are needed.

In the last few years, the use of smart functionalized systems has attracted much attention [9,11,12]. They are able to protect the drug from the degradative environment and to cross biological barriers, reaching intracellular compartments. Moreover, if a smart system is involved, release of the drug can be triggered by means of a change in a particular property of the medium—for instance, temperature, ionic strength, or pH. Once a drug is administered and released from the dosage form, its kinetic behavior largely depends on its chemical structure. However, if the drug is immersed in an NP, for example in a micelle, the physicochemical properties that will actually affect the distribution of the drug in the body are those of the latter. As a result, not only does this approach control release of the drug boosting therapeutic rates, but also any adverse effects are diminished [9,10]. Hence, it is possible to design NPs sensitive to, for example, the extracellular microenvironment and the acidic intracellular organelles of solid tumors. In this context, once they get in contact with the harmed tissue and respond to the low pH, they will deliver the drug, enhancing both tissue specificity and therapeutic outcomes [13].

However, the dynamic and reversible nature of micelle formation from dissolved polymers is a source of instability. To prevent their disruption by dilution, they can be modified by means of physical or chemical cross-linking, either in the shell or in the core, leading to stable unimolecular NPs able to keep their contents intact until a triggered stimulus occurs [14,15]. Of interest are the systems crosslinked by Diels Alder reaction in which furan-maleimide units or anthracene moieties are involved [16–20]. Thus, simple, fast, and reliable reactions

are required. Such reactions are the basis of click chemistry (CC) [21–24], the Diels-Alder reaction being one of them [7,17].

The overall aim of the present work is the preparation of aqueous dispersions of stable organic NPs, formed by self-assembly of tailor-made block copolymers, which may be used as smart, vectorizable, controlled drug delivery systems capable of responding under the right stimulus.

2. Experimental Section

2.1. General Methods

All chemicals used were purchased from Aldrich Chemical Co apart from Jeffamine D-230 polyetheramine, which was purchased from Hutsman. 2-Hydroxyethyl methacrylate (HEMA), *N*,*N*-diethylaminoethyl methacrylate (DEA), *N*,*N*-dimethylaminoethyl methacrylate (DMA), and furfuryl methacrylate (FMA) were passed through a basic alumina column and distilled before use. IR spectra were recorded on a Jasco FT/IR 4200 spectrometer equipped with ATR. Nuclear magnetic resonance (NMR) spectra were recorded at the CITIUS Service (University of Seville) at 300 K on either a Bruker Advance AV-500 or a Bruker AMX-500. Chemical shifts (δ) are reported as parts per million downfield from Me_4Si. Mass spectra were obtained using a Kratos MS80RFA instrument. Gel permeation chromatography (GPC) analyses were performed using a Waters apparatus equipped with a Waters 2414 refractive index detector and two Styragel® HR columns (7.8 x 300 mm^2) linked in series, thermostatted at 40 ºC, and using *N*,*N*-dimethylformamide (DMF) as the mobile phase at a flow rate of 0.5 mL/min. Molecular weights were estimated against methyl methacrylate standards. Fluorescence intensity was measured on a Varian Cary-Eclipse Fluorescence Spectrometer (Varian Iberica, Madrid, Spain) equipped with a xenon discharge lamp, two Czerny-Turner monochromators, and an R-298 photomultiplier tube detector. All the measurements took place in a standard 10 mm path-length quartz cell, and excitation and emission slits were both set at 5 nm. Fluorescence emission was measured at 380 nm with excitation wavelength of 360 nm or, for

CMC calculations, at 383 nm and 372 nm with excitation wavelength of 319 nm. The average diameter, size distribution (polydispersity index, PdI), and Z-potential of the samples were determined with a Malvern Zetasizer Nano ZS (Malvern Instruments, Malvern, UK) at 25 °C, with a particle size analysis range of 0.6 nm to 6 µm. The intensity of the scattered light (expressed in kilo counts per second) was measured by dynamic light scattering (DLS). The instrument is provided with 4 mW He–Ne laser (λ = 633 nm), digital correlator ZEN3600, and non-invasive backscatter (NIBS®) technology. Measurements were carried out at a scattering angle of 173º to the incident beam, and data analyzed using CONTIN algorithms (Malvern Instruments). Data for each dispersion were collected from at least three runs. Zeta-potential measurements were carried out with the same Zetasizer Nano ZS (Malvern Instrument), which measured the electrophoretic mobility of the sample from the velocity of the particles using a laser Doppler velocimeter (LDV). All the measurements were made at a fixed $C_{polymer}$ = 0.25 mg/mL. The solution pH was adjusted by the addition of 0.01 M HCl or 0.01 M KOH using an autotitrator. The morphology and distribution of the NPs were characterized by scanning electron microscopy (SEM) using a field emission HITACHI S5200 microscope operating at 5 kV, also used at the CITIUS Service (University of Seville). Before SEM observations, the dispersions were deposited and allowed to dry on a monocrystalline silicon support treated with oxygen plasma for 80 s to make it more hydrophilic. Fluorescent images were obtained with a ZEISS ApoTome epifluorescence equipment with motorized XY stage (maximum scanning area 130x85 cm), epifluorescence illumination Excite 120HXP with mercury-vapor lamp of 120 W and high-sensitivity monochrome camera Axiocam-506 to capture fluorescent images [of 1936x1460px sensor (3 Megapixel)]. DLS, SEM, and fluorescence measurements were all performed at the CITIUS Service (University of Seville). Measurement of absorbance of UV and visible light were conducted with an Agilent 8453 UV–visible spectrophotometer (Palo Alto, USA), equipped with diode array detection (DAD), and the data were the result of at least three measurements.

2.2. Synthetic procedures and micelle formation

Synthesis of pH-sensitive amphiphilic block-copolymer

In a typical experiment for the preparation of poly[($DMA_{25\%}$-$HEMA_{25\%}$)-*block*-($DEA_{45\%}$-$FMA_{5\%}$)] (**Scheme 1**), the initiator ethyl-2-bromo-2-methylpropionate (EBiB, 37 mg, 28 µL, 0.19 mmol), HEMA (0.92 mL; 7.59 mmol), and DMA monomer (1.53 mL, 7.59 mmol) were dissolved in 2.45 mL of pure methanol. To this degassed solution the 2,2'-bipyridyl ligand (bipy, 74 mg; 0.48 mmol) and the CuBr catalyst (27 mg; 0.19 mmol) were added, while stirring, at 25 °C, to produce a 50% (w/v) dark brown solution. The reaction proceeded for 2 h and then an aliquot was taken out immediately before the addition of the other monomers.

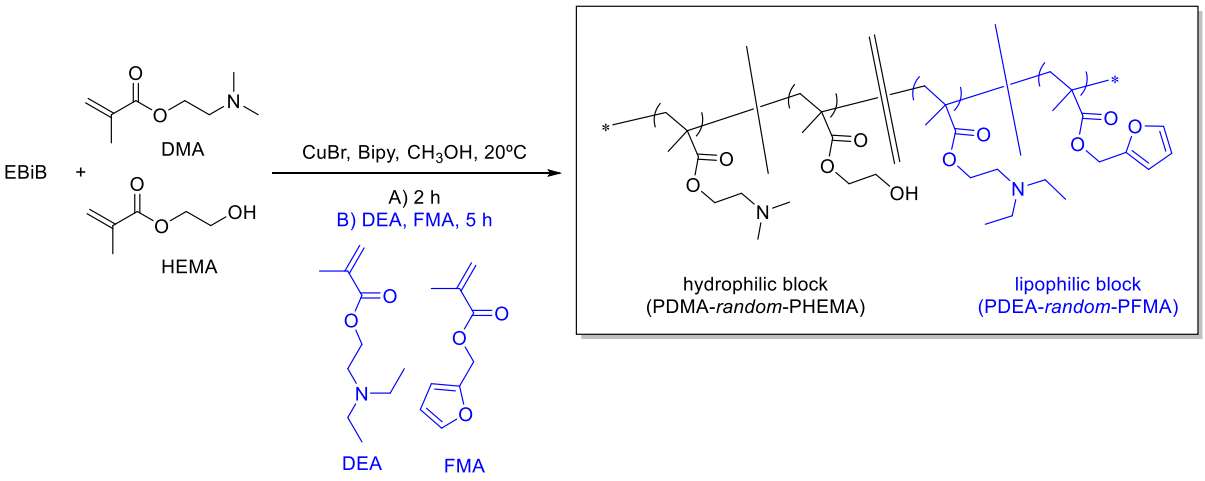

Scheme 1. General structure of synthesized methacrylate-based *block*-copolymers and cross-linkers.

This aliquot was analyzed by ^{1}H NMR and GPC in order to obtain both the molecular weight (M_n) and the molar percentage composition of the first block. Next, a degassed solution of DEA (2.3 mL; 13.67 mmol) and FMA monomer (0.234 µL; 1.52 mmol) in methanol (2.55 mL) was added and the reaction was allowed to proceed for a further 24 h. Purification was achieved by stirring the reaction dispersion with silica in methanol and later passing it through a diatomaceous earth column to remove the Cu(II) catalyst joined to the silica gel. The resulting colorless solution was evaporated under vacuum to produce the white copolymer in high yield (4.3 g, 85%). GPC data: M_n = 34,700; M_w = 45,100; M_w/M_n = 1.3. Experimental

copolymer composition (determined by ^{1}H NMR): ($DMA_{31\%}$-$HEMA_{19\%}$)-*block*-($DEA_{45\%}$-$FMA_{5\%}$).

IR, ν, (cm^{-1}): 3420 (O-H), 2964 (=C-H st, furan), 2932 (-C-H st), 1722 (C=O st), 1453, 1383 (γ ring skeleton furan), 1264, 1240 (C-O st ester), 1141 (C-N st amine). ^{1}H NMR (DMSO-d_6,500 MHz), δ (ppm): 7.67-6.47 (m, 3 H, furan); 4.98 (s, 2H, $COOC\underline{H}_2$-furan, FMA); 4.82 (s, 1 H, OH, HEMA); 4.51-4.32 (m, 4H, $COOC\underline{H}_2$, DMA and DEA), 3.91-3.82 (m, 6H, $COOCH_2C\underline{H}_2$, DMA, DEA, HEMA); 3.59 (bs, 2H, $COOC\underline{H}_2$, HEMA); 2.26-2.11 (m, 10 H, $N(C\underline{H}_3)_2$, DMA and $N(C\underline{H}_2CH_3)_2$, DEA); 2.03-1.62 (m, 8 H, $-C\underline{H}_2-C(CH_3)-$, DMA, HEMA, FMA, DEA); 1.06-0.58 (m, 18 H, $-CH_2-C(C\underline{H}_3)-$, DMA, HEMA, FMA, DEA, $N(CH_2C\underline{H}_3)_2$, DEA).

^{13}C NMR (DMSO-d_6, 125 MHz), δ (ppm): 177.1 (C=O), 137.3 (1C, furan); 111.3 (2C, furan); 66.5-62.7 (3C, $COOCH_2\underline{C}H_2$, DMA, DEA, HEMA); 59.2 ($COO\underline{C}H_2$, HEMA); 58.3 ($COO\underline{C}H_2$-furan, FMA); 55.8 ($COO\underline{C}H_2$, DMA and DEA); 54.9 ($-\underline{C}H_2-C(CH_3)-$, DMA, HEMA, FMA, DEA); 45.4 ($N(\underline{C}H_3)_2$, DMA and $N(\underline{C}H_2CH_3)_2$, DEA); 18.0 ($-CH_2-C(\underline{C}H_3)-$, DMA, HEMA, FMA, DEA); 11.7-11.9 ($N(CH_2\underline{C}H_3)_2$, DEA).

Preparation of cross-linkers

The synthesis of the bisdienophile 1,8-dimaleimide-3,6-dioxaoctane (DMDOO) has been described elsewhere [7]. The same procedure was followed for the preparation of the bismaleimide derived from Jeffamine D230 (DMJF) and is described next.

In brief, a solution of Jeffamine D-230 polyetheramine (6.9 g, 30 mmol) in 15 mL of DMF and maleic anhydride (7.9 mL, 120 mmol) in 30 mL of DMF were mixed carefully in order not to exceed 80 ºC, and the reaction mixture was stirred for 20 min at 75 ºC. Then acetic anhydride (22.7 mL, 240 mmol), nickel (II) acetate tetrahydrate (0.119 g, 0.48 mmol), and triethylamine (3.3 mL, 24 mmol) were added at once and stirred for 1 additional hour at 75 ºC. To quench the reaction, 70 mL of water were added and the mixture was stirred for 5 min.

The aqueous phase was extracted with dichloromethane (5 x 100 mL), and the obtained residue was evaporated to 300 mL. To the combined organic phases, 70 g of silica were added, and the mixture was filtered through a short pad of celite in order to get rid of the salts. The pad was washed with dichloromethane, and the solution was evaporated to yield a final residue that was purified via column chromatography (*tert*-butylmethyl ether-hexane from 9:1 to 1:0) to give the title compound as a pale yellow oil (4.1 g, 35%).

IR, ν, (cm^{-1}):3099 (=C-H st), 1703 (C=O st), 1106 (O-CH_2 st), 692 (C=C alkene cys).^{1}H NMR ($CDCl_3$, 500 MHz) δ (ppm): 6.65 (s, 4 H, CH=CH), 4.50-4.22 (m, 2 H, -CH), 3.93-3.20 (m, 10H, -CH, -CH_2), 1.33-1.27 (m, 6H, -CH_3), 1.10-0.90 (m, 6H, -CH_3). ^{13}C NMR ($CDCl_3$, 125 MHz) δ (ppm) 171.0, 170.9, (C=O), 134.0, 133.9 (C=C), 74.9, 74.8, 46.7, 46.2, (-CH), 74.6, 71.3, 69.3, 69.2, (-CH_2-), 17.0, 16.9, 16.7, 14.9 (-CH_3).

HRFABMS: Calculated molecular weight for $C_{20}H_{28}O_7Na$ [$(M + Na)^+$] : 431.1794; experimental molecular weight: 431.1719.

Formation of micellar nanoparticles through self-assembly process

For illustrative purpose, the recipe to prepare a micellar dispersion at polymer concentration 0.25 mg/mL is described next. The poly[($DMA_{31\%}$-$HEMA_{19\%}$)-*block*-($DEA_{45\%}$-$FMA_{5\%}$)] copolymer (0.063g) was dissolved in THF (10 mL, final polymer concentration: 6.3 mg/mL) at 25 °C and the solution was added dropwise over 200 mL of double-distilled water. The chains underwent self-assembly to form a dispersion of well-defined micelles with the DEA-FMA blocks forming the dehydrated micelle cores. Next, the nanoparticle dispersion was diluted by the addition of the required amount of water to get the targeted volume (250 mL, final polymer concentration = 0.25 mg/mL) and gently stirred for 72 h.

Formation of stabilized core cross-linking nanoparticles

To obtain stabilized nanoparticles by cross-linking reactions, the polymer concentration, the cross-linking agent (either DMDOO or DMJF), and the degree of cross-linking aimed at (for example, 10% or 20%) were selected. Each cross-linking assay was carried out as described next: a solution of the selected bisdienophile (either DMDOO or DMJF, in DMSO, 1 mg/mL) was mixed with an exact volume of freshly prepared THF-polymer solution. The exact volume of double-distilled water needed to achieve the target concentration was poured into a round-bottom flask provided with a stirring bar, and the mixture of the selected cross-linker and the polymer was added dropwise. The amount of cross-linker was calculated on the basis of FMA units. The dispersion was then gently stirred for 72 h at 25 ºC. For comparative purposes, a micellar dispersion of the same polymer concentration was prepared.

Stability of nanoparticles

To study the stability of the nanoparticles, two different methods were carried out:

(a) 10 mL of the selected dispersion was poured into a round-bottom flask and HCl 0.3 M was added dropwise with stirring until a final pH of 3.0. The mixture was gently stirred at 25 ºC until the pH values remained stable for at least 24 hours. Then, the aqueous dispersions were studied by means of DLS, Z-potentials, and SEM.

(b) The NPs from the selected dispersion were separated from the aqueous phase by ultracentrifugation at 35 000 rpm for 30 min. The NPs were then dissolved in *N*,*N*-dimethylformamide (DMF, final polymer concentration = 0.25 mg/mL) at 25 °C and gently stirred for 72 h. The presence (or not) of the NPs in the organic dispersions was ascertained by DLS.

2.3. Characterization of self-assembled nanoparticles

Determination of the critical micelle concentration (CMC)

To determine the CMC, two different methods were used: (a) the well-established pyrene method, and (b), the CMC was calculated by means of visible spectroscopy (at 600 nm) taking advantage of the typical bluish color exhibited by micelle aqueous solutions.

For both procedures, a stock solution of the *block*-copolymer (100 mL, 0.45 mg/mL) was prepared by dissolving it (0.045 g) in THF (4.5 mL) at 20 ºC. The solution was added dropwise over 90 mL of double-distilled water under stirring and the final polymer solution volume was adjusted by addition of the required amount of distilled water. After 72 h, aqueous dilutions were prepared in the 0.3375 mg/mL – 0.0067 mg/mL concentration range, samples incubated at 25 ºC (48 h).

Method (a): Pyrene fluorescence intensity

An aqueous solution of pyrene (1.0 mL, 12 µg/mL) was added dropwise to 9 mL of the each polymer dilution under stirring (final pyrene concentration = 1.2 µg/mL) and the mixture was gently stirred for 6 days. The fluorescence emission peaks I_I and I_{III} at 372 nm and 383 nm respectively, were measured and the ratios I_{III}/I_I represented against the polymer concentrations, being the inflection point the value corresponding to the CMC. Calculated CMC: 0.085 mg/mL

Method (b): Visible spectroscopy (600 nm)

The absorbance of the visible light of the prepared polymer dilutions was measured at 600 nm using distilled water as a blank. The data for each dilution were collected from at least three runs. Absorbance was plotted as a function of the copolymer concentration [(mass of polymer (mg)/volume solution (mL)] and the CMC was established as the intersection between the two straight trend lines from the analyses of the lower-concentration polymer solution and the upper-concentration polymer solution, leading to a CMC = 0.078 mg/mL.

Microscopy studies (SEM, and fluorescence correlation spectroscopy)

In order to determine the NP size distribution and to compare the resulting data with DLS results, statistical analysis was also conducted from SEM and fluorescence images. For that purpose, an algorithm based on an adaptive thresholding method was used [25]. This approach, which makes use of local threshold evaluation, allows particles to be detected automatically and/or manually and characterized with greater accuracy than when using more-conventional methods in which a global threshold is used. The detected particles' boundaries were then fitted by ellipses defined by their major and minor axis a and b, respectively, and the size of each NP was determined using the mean geometric diameter of the fitted ellipse $d = \sqrt{ab}$. Finally, the mean particle size dm was obtained by fitting the size distribution with a log-normal function defined as

$$f(d) = \frac{1}{d\beta\sqrt{2\pi}} \exp\left[-\left(\frac{\ln\left(\frac{d}{d_m}\right)}{\beta\sqrt{2}}\right)^2\right] \qquad \text{Equation 3}$$

where β represents the relative polydispersity [26]. It is worth mentioning that the use of the adaptive thresholding algorithm to detect the particles was applied with special care in order to remove possible clusters of several NPs detected from the statistical analysis, and to keep only individual particles that are the most representative of the size distribution within the samples.

2.4. Drug loading

Loading of lipophilic molecules into nanoparticles

An aqueous solution of pyrene (1.0 mL, 12 µg/mL) was added dropwise to 9 mL of the micelle dispersion under stirring (final pyrene concentration = 1.2 µg/mL; final polymer concentration = 0.225 mg/mL). The mixture was gently stirred for 6 days. The process was conducted with the five micellar dispersions prepared: one non-cross-linked and four with the

core stabilized by click reactions (with DMDOO, DMJF, 10% or 20%). Similarly, 1 mL of the pyrene solution (12 µg/mL) was added over distilled water (9 mL), and the resultant sample (LMa-0) was used for comparison purposes.

Kinetic studies of loading capacity of the prepared NPs for a therapeutic agent, pilocarpine, were carried out as follows: 5 mL of the micellar dispersion was mixed with an aqueous pilocarpine solution (5 mL, pilocarpine concentrations 0.2, 0.4, and 0.8 mg/mL; final pilocarpine concentrations = 0.1, 0.2, 0.4 mg/mL; final polymer concentration = 0.125 mg/mL), gently stirred, and the absorbance was measured at the maximum UV absorption of pilocarpine: 215 nm. Measurements were made at predetermined intervals from time = 0 to time = 6 days. The original micelle dispersion was used as blank in each trial. For comparative purposes, a pilocarpine solution was prepared: the same volume of the pilocarpine solution (5 mL, pilocarpine concentration 0.2, 0.4, or 0.8 mg/mL) was added to 5 mL of double-distilled water in order to use it as a reference (final pilocarpine concentration = 0.1, 0.2, and 0.4 mg/mL). The load capacity of the NPs was determined by comparing the absorbance values at 215 nm of the reference pilocarpine solution prepared *ex profeso* with those coming from the loaded-micelle dispersions.

Prior to the analysis, calibration was made with pilocarpine standard aqueous solutions (5–75 µg/mL) at 215 nm. The polynomial calibration equation for pilocarpine was obtained as follows:

$$C(\mu g\, mL^{-1}) = \frac{A + 0.0217}{0.023} \qquad \text{Equation 1}$$

where C denotes the pilocarpine concentration in solution, and A represents the absorbance at 215 nm. The accumulative pilocarpine uptake was estimated as follows:

$$\text{Cumulative pilocarpine uptake}(\%) = \frac{P_t}{P_0} \text{x } 100 \qquad \text{Equation 2}$$

where P_t and P_0 represent the amount of pilocarpine absorbed at time *t* and the initial amount of pilocarpine added to the micelle dispersion, respectively.

Stimulus-response release of selected molecules from nanoparticles

An aliquote (2 mL) of each pilocarpine-loaded micellar solutions (0.125 mg/mL) was transferred to a mini-dialysis tube (1 kDa cut-off, GE Healthcare) and immersed in a beaker containing a stirring bar and 10 mL of a buffer solution at pH 3.0 (citrate-buffered saline) or at pH 7.4 (phosphate-buffered saline) The system was stirred at 25 ºC and, at each predetermined time, 0.2 mL of the incubated solution was removed and replenished with an equal volume of the same acidic solution. The release profiles were determined by measuring the absorbance at a wavelength of 215 nm.

3. Results and Discussion

3.1. Preparation of stabilized nanoparticles based on amphiphilic block-copolymer

Synthesis of furan-containing block-copolymers and cross-linkers

First, the synthesis of amphiphilic methacrylate-based *block*-copolymers capable of self-assembly into stimulus-response NPs was addressed. For the further stabilization of the NPs, the cross-linking of either the micellar core or shell would need the presence of reactive functional groups in either the hydrophobic or hydrophilic blocks, respectively. One major drawback in the synthesis of conventional shell cross-linked micelles is that the reaction must be carried out at high dilution in order to avoid extensive intermicellar cross-linking. In the reported cases where the shell was successfully cross-linked, a steric stabilizer was present and the intermicellar reactions were prevented [27]. These drawbacks can be avoided if the core is cross-linked instead, since the hydrophilic segment will behave as a steric stabilizer in the process [28–30].

Also of interest is the presence of functional groups in the NPs, available for the inclusion of recognition ligands, useful for active vectorization toward specific tissues and cells, if required. As a reliable option, the hydroxyl groups are biologically compatible and also of use in many reactions.

The selection of monomers was as follows: as hydrophilic monomers, HEMA and DMA were chosen, and for the lipophilic segment, FMA and DEA monomers. Thus, the polymers would enclose (a) pH-sensitive units (tertiary amine groups in DMA and DEA) on both the hydrophobic and the hydrophilic segments, leading to pH-sensitive polymers; (b) furan rings in the lipophilic block (in FMA), able to subsequently cross-link *via* Diels-Alder reaction with selected bisdienophiles; (c) hydroxyl functional groups (in HEMA moieties) in the hydrophilic block, which would be available for vectorization with the appropriate marker agents, if required (**Scheme 1**).

The well-known "living" polymerization technique atom transfer radical polymerizations (ATRP) [5,31] was used, and excellent control over the compositions and polydispersities of the materials was achieved. For the preparation of the polymers, the constituent monomers of both blocks were added in two selected times of the process, so that the hydrophilic block would be synthesized first, and the addition of the monomer mixture, DEA and FMA, was done when ca. 95% of the hydrophilic monomers was consumed (data obtained from ^{1}H NMR). The composition of the hydrophilic block was determined by examining an aliquot extracted from the reaction medium before the addition of the hydrophobic monomers. Thus, the composition (in mole percentage) of each repeating unit was calculated by ^{1}H NMR. Similarly, and using those values as reference, the overall copolymer composition was revealed.

The peaks from the ^{1}H NMR spectra selected to reveal the copolymer composition were those corresponding to the methylene group adjacent to the ester group (-COOC$\underline{H_2}$-): for the first block, the integrals of the peaks at 4.44 ppm and 3.59 ppm, corresponding to DMA and HEMA respectively, were compared. For the second block and, hence, for the final copolymer composition, the combined information extracted from the analyses of the first block, and from the integrals of the peaks at 4.51-4.32 ppm and 4.98 ppm, corresponding to DMA+DEA and FMA respectively, rendered the final copolymer mole composition. It was found that the only polymer able to spontaneously self-assemble into micellar NP in aqueous media was the polymer with the experimental composition [(DMA$_{31\%}$-HEMA$_{19\%}$)]-*block*-(DEA$_{45\%}$-FMA$_{5\%}$)] (GPC data: M_n = 34,700; M_w = 45,100; M_w/M_n = 1.3).

The cross-linking agents prepared were two bismaleimides capable of performing Diels-Alder reactions with the furan rings present in the hydrophobic block copolymer. For that purpose, two starting diamines were used: 1,8-diamino-3,6-dioxaoctane and Jeffamine D-230, leading to their respective bisdienophiles, DMDOO and DMJF (**Scheme 2**) by a gram-scale reaction in good to modest yields (72% and 35%, respectively). Commercial Jeffamine D-230 is a mixture of several diamines differing from each other in the number of propylene oxide units present in the spacer. DMDOO has been described in a previous work [7], and DMJF was synthesized following the same procedure (a detailed characterization of the new cross-linker is included in the experimental part). Although in the case of DMJF a mixture of bisdienophiles is present as a logical consequence of the nature of the starting material, DMDOO and DMJF are quite similar in size and structure; however, DMJF is less polar than DMDOO due to the more hydrophobic nature of the spacer (oligopropylene oxide) present in the former than that (oligoethylene oxide) in DMDOO.

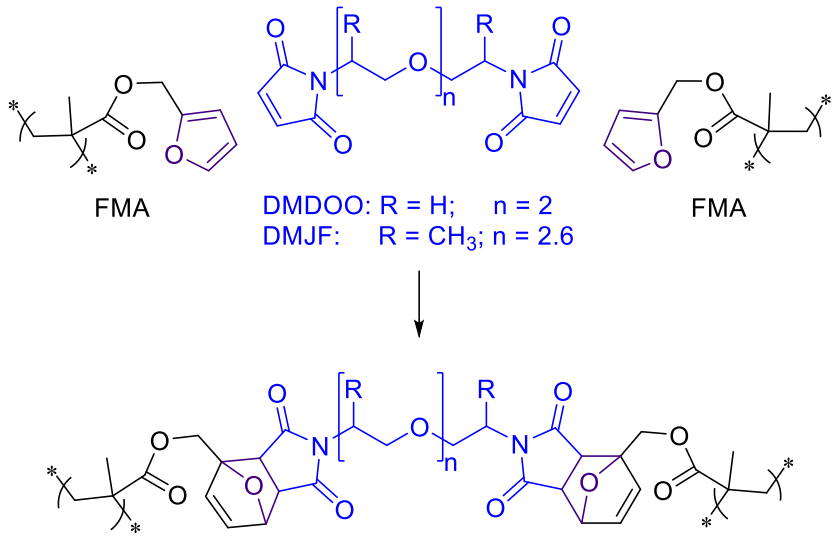

Scheme 2. Core cross-linking reaction between DMDOO or DMJF and FMA residues from the micelle core.

The formation of Diels-Alder adducts from such bisdienophiles with furan rings has previously been confirmed by NMR studies and mass spectrometry, either by fast atom bombardment (FAB) or chemical ionization (CI). The latter technique, along with calorimetric studies, confirmed the reversibility of adduct formation at temperatures close to 85 °C [7].

Nanoparticle formation in aqueous media

The self-assembly of FMA-based copolymers in aqueous media was then studied, as well as the critical micelle concentration (CMC). The properties of the generated nanoparticles, such as size, polydispersity, and shape [32,33] were explored by means of various techniques, including scanning electron microscopy (SEM) and dynamic light scattering (DLS).

At neutral pH, well-defined micelles were formed in aqueous solution with the DEA-FMA blocks forming the dehydrated micelle cores, leaving the hydrophilic blocks in the outer part of the nanoparticles in contact with the aqueous medium. The soft bluish appearance usually

found when light is scattered from nanosized particle dispersions was observed, suggesting the NP formation. By means of DLS experiments it was found that a nearly monodisperse NP dispersion was achieved when the polymer concentration was 0.25 mg/mL (PDI = 0.12; D_h = 205 nm), whereas at higher polymer concentrations (>0.45 mg/mL), the NPs were clustered, resulting in polydisperse, micron-sized systems. A detailed study of the NPs is described below.

Critical micelle concentration (CMC)

The sensitivity of the pyrene fluorescence intensity to the solvent polarity is widely used for the determination of the CMC of micellar systems. The CMC was determined from the pyrene fluorescence intensity, especially from the intensity ratio at two vibronic bands in the monomer emission: band at peak I (372 nm) and peak III (383nm) as function of the polymer concentration [34] (Figure S1, Supplementary material). The CMC was estimated to be 0.085 mg/mL. Above that concentration, the polymer chains self-assemble, leading to NP dispersions.

The CMC was also calculated by visible spectroscopy. The absorbance of aqueous polymer solutions at 600 nm was plotted against polymer concentration (mg/mL). The plot (Supplementary material, Figure S1) showed that the polymer solutions with concentrations ≤ 0.05 mg/mL did not experience a marked absorbance, similarly to dissolved polymers. However, when the concentration of the polymer solution studied stood at 0.11 mg/mL or higher, a change in trend occurred and the absorbance of the dispersions rose substantially in line with the concentration. Furthermore, in the latter more-concentrated dispersions the typical bluish appearance of this type of dispersion was observed. The CMC was obtained from the cutoff point or intersection of the two straight lines obtained by the trend analyses of polymer solutions at lower and higher concentrations (CMC = 0.078 mg/mL). Consistent

values of the CMC were obtained by both methods and they were closely comparable to each other (0.085 mg/mL and0.078 mg/mL).

Stabilization of nanoparticles via core cross-linking reactions

Building on the experience in both formation of micelles stabilized by steric agents [32] and studies of the Diels-Alder reactions on polymers functionalized with furfuryl groups [7], the stabilization of the NPs by cross-linking their core *via* Diels-Alder reactions was proposed. Both the degree of cross-linking in the micellar core and the nature of the cross-linker were the parameters to fit in these assays in order to track the impact of these two variables on the stability and drug loading capacity of the NPs. As cross-linkers, DMDOO and DMJF were chosen, and the degree of cross-linking studied ranged from 10% to 50%. Thus, furan rings present in FMA units would react in pairs with the two maleimide groups from the selected bisdienophile—either DMJF or DMDOO (Scheme 2)—generating a cross-linked core which is able to impart stability to the NP.

To carry out the cross-linking, the addition of a solution of the selected bisdienophile in DMSO (bisdienophile concentration = 1 mg/mL) into the micellar dispersions (polymer concentration 0.45 mg/mL) was initially attempted. The target cross-linking degrees stood at 25% and 50%. The five different samples—designated M1-X—are distinguished from each other depending on the cross-linker used—if any—as well as the amount of bisdienophile added, in order to achieve the targeted degree of cross-linking (Table S1, Supplementary material). In these assays, the presence of a precipitate was observed in every case, probably due to the insolubility of the bisdienophile and/or of the adduct formed.

To overcome this drawback, for the next assays reductions were made in both the polymer concentration (to 0.25 mg/mL) and degree of cross-linking (to 20% and 10%, samples M2-X, **Table 1**). At the same time, the polymer and the bisdienophile came into contact before the

micelle formation. Bluish dispersions were achieved with the absence of any precipitate in the reaction flasks. The samples M2-X were studied by DLS and SEM (detailed information recorded below) and some stability studies in acidic media (samples M3-X, Table 1) and in DMF (samples M4-X, Table 1) were carried out next.

Table 1. Values of PdI and average size (D_h, nm) of the NPs prepared at polymer concentrations 0.25 mg/mL, in aqueous media at neutral pH (M2-X) and acid pH (M3-X) and in DMF (M4-X).

Sample	Bisdienophile	Z-average (nm)	PdI	Peak No.	Population 1		Population 2	
					Size (± SD) (D_h.nm)	%	Size (± SD) (D_h.nm)	%
pH 7.0								
M2-1	…	177	0.12	1	205 (± 81)	100	--	--
M2-2	DMDOO 20%	108	0.33	2	129 (± 74)	95	4645 (± 814)	5
M2-3	DMDOO 10%	83	0.28	2	114 (± 75)	95	4685 (± 790)	2
M2-4	DMJF 20%	87	0.38	2	149 (± 139)	95	4528 (± 867)	2
M2-5	DMJF 10%	237	0.45	3	96 (± 26)	23	400 (± 186)	73
pH 3.0								
M3-1	…	218	0.16	1	260 (± 104)	100	--	--
M3-2	DMDOO 20%	245	0.33	2	28 (± 6)	6	199 (± 55)	94
M3-3	DMDOO 10%	196	0.24	1	262 (± 126)	100	--	--
M3-4	DMJF 20%	177	0.36	2	45 (± 12)	9	224 (± 80)	91
M3-5	DMJF 10%	206	0.22	1	242 (± 101)	100	--	--
DMF								
M4-1	…	--	--					
M4-2	DMDOO 20%	220	0,27	2	256 (± 133)	96	4875 (± 691)	4
M4-3	DMDOO 10%	178	0.36	2	209 (± 115)	93	7397 (± 927)	7
M4-4	DMJF 20%	164	0.45	2	212 (± 150)	93	4669 (± 806)	7
M4-5	DMJF 10%	414	0.45	3	150 (± 40)	20	659 (± 319)	74

The success of the core cross-linking assays, with both bisdienophiles (DMDOO and DMJF) at 10% and 20% degree of cross-linking, was confirmed by two methods. First, the polymer dispersions were acidified to pH 3.0 and studied by DLS, SEM, and zeta-potential. To simplify the discussion, the nomenclature of the samples changed to M3-X when these resistance tests were conducted. Thus, when some drops of a 0.03 M solution of hydrochloric

acid were added, the basic units of the polymer were expected to be protonated [35]. In the event that the micelles were not cross-linked, the polymer chains would fly apart by charge repulsion and a molecular polymer solution would be obtained. Conversely, if cross-linking was successfully achieved, the protonation in the core would not be able to break the three-dimensional structure of core cross-linked NPs. Moreover, in acidic media, micellar structures with hydrated cores might be obtained, with the consequent boost in hydrophilicity.

The experimental DLS data first confirmed the presence of NPs in the acidic solutions, in all cases, even in the non-cross-linked systems, which remained stable under those experimental conditions. In addition, aqueous electrophoresis studies were conducted on each of the NPs at pH 3.0 as well as on the non-cross-linked sample, in order to assess their relative colloidal stabilities. At low pH these dispersions each possess positive zeta-potentials ranging from +49 mV to +55 mV (Supplementary material, Figure S2), confirming protonation of the weakly basic amine residues [8].

Another set of assays were conducted in which DMF, a good solvent for the two blocks of (PDMA-*random*-PHEMA)-*block*-(PDEA-*random*-PFMA), was used as a solvent to disperse the core cross-linked micelles previously isolated from the aqueous dispersion. Interestingly, DLS studies (M4-X, Table 1) showed that the micelles in DMF can still maintained their nanostructures, indicating that the covalent cross-linking of a hydrophobic block can boost the stability of the micelles considerably. In addition, an increase of the hydrodynamic volume of the NP was observed, suggesting the incorporation of DMF in the core of the NPs.

3.2. Characterization of the self-assembly nanoparticles

Studies of size, size distribution, and geometry of NP

For the present study, data obtained by DLS of average particle size (hydrodynamic diameter, D_h, in nm) of each population of NP in the sample—if more than one population is present—and polydispersity index (PdI) are collected in Table 1.

The data of the first NP-stabilization trials (M1-X) are recorded in Table S1 (Supplementary material). In general terms, when the polymer concentration stood at 0.45 mg/mL or higher, a high degree of cross-linking was targeted (50% or 25%), the presence of polydisperse systems with 2 or 3 NP populations was observed (one of average size lower than 100 nm (60 nm to 83 nm) and another around 340 nm (317 nm to 438 nm)), heralding a certain tendency to aggregate formation. Furthermore, the presence of a population of micron-sized particles in every cross-linked sample is responsible for the large polydispersities. This trend is considerable in samples M1-3 and M1-5, where the cross-linking degree stood at 25%.

The NPs formed at lower polymer concentration (from M2-1 to M2-5, aimed degree of cross-linking 20% or 10%), stabilized or not, showed a higher particle size than those from the more concentrated dispersions M1-X. Thus, the average particle size found for the non-cross-linked sample was about 200 nm (M2-1) whereas this size decreased when the core was cross-linked (from 95 nm to 150 nm), suggesting that the cross-linking process involved an increase in density of the NP core. Conversely, sample M2-5 displayed a different trend than the others, with an average main population of 400 nm, corresponding to some clusters, as can be observed in the SEM images. Furthermore, the NPs remained without change for a lengthy period of time (> 5 months) and at a broad range of temperatures (from 5 ºC to 40 ºC), which verifies their stability in a number of conditions.

The experimental data of NPs in the acidic solutions displayed average D_h ranging from 199 nm to 262 nm—values higher than those from the same samples at neutral pH (Table 1). This is in agreement with the hypothesis on the change from amphiphilic NPs, at acid pH, into

fully water-soluble structures with hydrated cores. At pH 3.0, the loss of the aggregates observed at neutral pH in sample M2-5 (see data for sample M3-5, Table 1) was also achieved, together with a slight reduction in PdI, probably due to the repulsion between charged micelles.

These data were corroborated with the SEM images from selected samples (Figure 1, 2 and 3). **Figure 1** shows two SEM micrographs representative of the non-cross-linked micellar structures of the M2-1 and M3-1 samples. In both cases, these images clearly evidence that the micelles are almost spherical with a smooth surface, and—hence—stable spherical nanosized non-cross-linked micellar structures were displayed in both neutral and acid media. According to the size distributions obtained from statistical analysis of a set of SEM images, the mean size of the NPs in the M3-1 sample is higher (dm = 127 nm) than in the M2-1 sample (dm = 95 nm). This trend is in good agreement with DLS results.

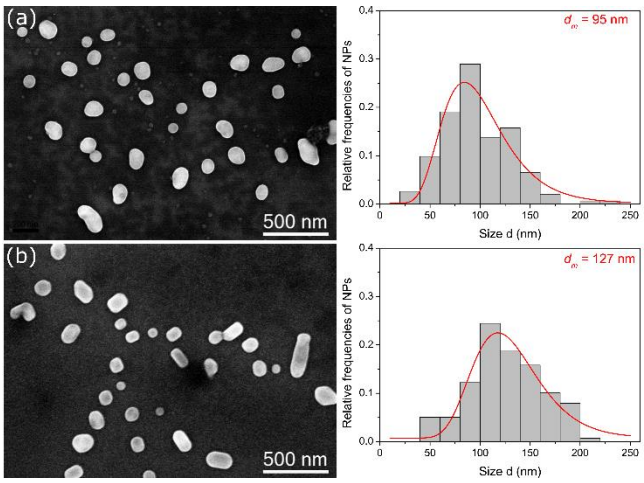

Figure 1. SEM micrographs and size distributions extracted from statistical analysis performed on various SEM images for (a) sample M2-1 at pH 7.0 and (b) sample M3-1 at pH 3.0. The curves correspond to the fit of the distributions using a log-normal function.

The SEM images representative of the cross-linked structures under neutral pH conditions are shown in **Figure 2 (a)**. The morphology of the NPs observed in the images confirms that nanosized cross-linked structures remain stable. According to the size distribution analysis, samples M2-3, M2-4, and— especially—M2-2, contain smaller NPs than for the non-cross-linked micellar structure M2-1. A similar trend is observed by DLS. In the case of sample M2-5, the SEM images indicate a strong agglomeration of particles, which makes the extraction of a reliable NP size distribution impossible. An estimation of the NP size range as between about 80 nm and 100 nm can however be obtained by measuring the diameter of some NPs in the image.

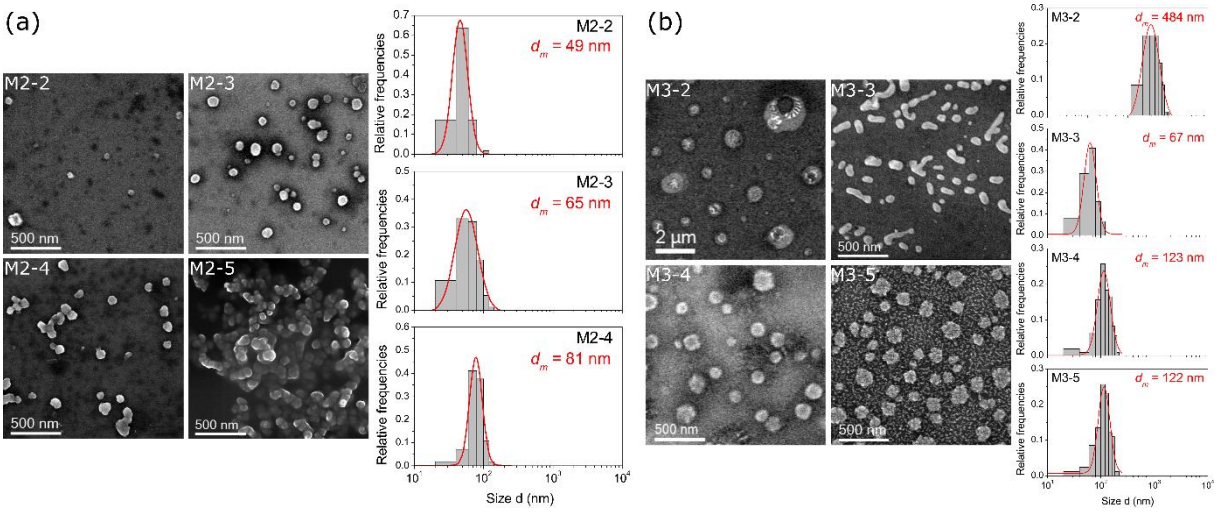

Figure 2. SEM micrographs of the core cross-linked samples at neutral pH (a) and at acid pH. (b). Size distributions extracted from statistical analysis performed on various SEM images are also plot. The curves correspond to the fit of the distributions using a log-normal function. In the case of sample M2-5, analysis of the size distributions has not been performed because the NPs are strongly agglomerated.

Figure 2 (b) presents SEM images representative of the core cross-linked structure in acid pH. The NP sizes in samples M3-4 and M3-5 (dm = 123 nm and dm = 122 nm, respectively) are very similar to that of the non-cross-linked micellar structure M3-1, while the NPs observed

in sample M3-3 are smaller (dm = 67 nm). It is important to mention that sample M3-2 contains structures substantially larger than (dm = 484 nm), and has a morphology significantly different from, the rest of the samples.

The evolution of the mean NP size determined by DLS (Z-average, main population) and SEM are compared in **Figure 3**. As a general trend, the size evolution is similar using the different measurement methods, especially for samples M2. However, the values obtained by SEM are generally lower than those obtained by DLS. This difference can be attributed to the fact that DLS tends to overestimate the mean size in the presence of particle agglomerates (even by a small amount), while diameters determined by SEM have to be considered the lower limits of particle size [36].

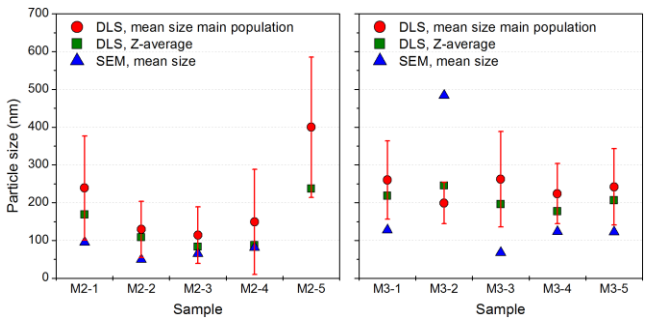

Figure 3. Comparison of the mean NP size determined by DLS and SEM for sample M2 (pH 7.0) and M3 (pH 3.0).

3.3. Loading of lipophilic molecule / drug into nanoparticles

The loading of lipophilic molecules by these systems was evaluated next; the encapsulation studies of a fluorescent molecule, pyrene [37], and a drug, pilocarpine, were conducted by means of UV-vis and fluorescence spectroscopies, and fluorescence microscopy.

Loading of pyrene

Pyrene is a polyaromatic hydrocarbon that presents an ensemble of fluorescence emission peaks in the range from 375 nm to 405 nm. It is exquisitely sensitive to polarity of the probe's microenvironment, and consequently could be used for the analysis of its surroundings [38]. Thus, once the fluorescent molecule is immersed into a hydrophobic environment, such as the core of the prepared NPs, a boost in the fluorescence emission is expected. This phenomenon was also found in other fluorescent molecules such as gatifloxacin, an antibiotic of the fourth-generation fluoroquinolone family; Ocaña *et al.* reported a final fluorescence intensity enhancement of about 75% by this method [39].

To carry out the incorporation of pyrene, the samples were prepared by the addition of an aqueous solution of pyrene into the micelle dispersion. The mixtures were gently stirred on a rotor for 6 days and the fluorescence emission was measured ($\lambda_{absorption}$ = 338 nm; $\lambda_{emission}$ = 380 nm) at four established times to track the evolution of data (LMa-1 to LMa-5, Table S2 of Supplementary material and **Figure 4**). Sample LMa-0 corresponds to a dilute solution of pyrene (1.2 μg/mL); even though this sample contained the maximum concentration of free pyrene, it showed a weak native-emission signal in aqueous medium, in agreement with the polar aqueous environment.

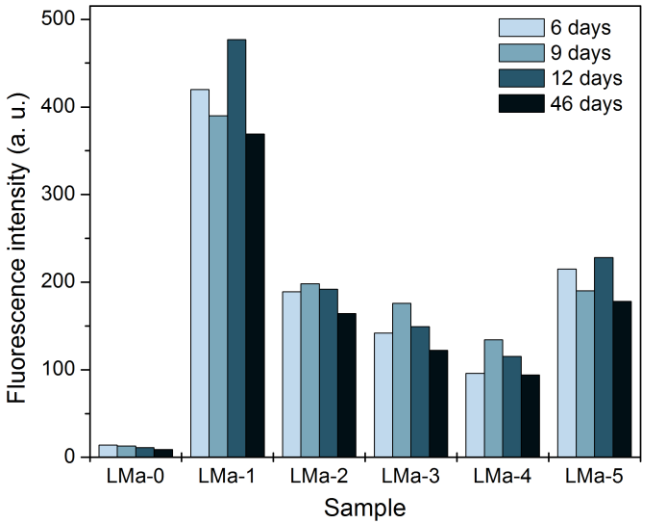

Figure 4. Fluorescence-emission data at 380 nm (arbitrary units) of pyrene loading tests at selected periods of time.

From the figures recorded in Table S2, it was inferred that pyrene was successfully embedded in the NPs [39] in all the samples; the fluorescent emission rose to values far above those for aqueous pyrene solutions (from 9.5 to 36.1 times higher), confirming the non-polar surroundings of the lipophilic molecule in the NPs.

Some additional information was revealed: more-apolar surroundings were provided by the non-cross-linked micelles, with emission values that doubled those from cross-linked NPs.

Fluorescence microscope images from pyrene-loaded samples were taken. It was found that the micellar size of non-cross-linked micelles rose substantially compared with that of non-cross-linked, pyrene-free micelles (**Figure 5**). *A priori*, the only NPs able to substantially change their size are the non-cross-linked samples (samples 1 in each assay) as the dynamic equilibrium between unstabilized NPs and the polymer chains (unimers) allows the reorganization of those structures. From the analyses of the images, this phenomenon was found only in sample LMa-1, with an increase in size close to 10-fold compared with M2-1 (dm = 1.27 μm). Sample M2-1 seemed to have evolved into thermodynamically more-stable

microparticles with pyrene embedded in the core (LMa-1). Conversely, this phenomenon was not found when pyrene was incorporated into the other NPs (from LMa-2 to LMA-5). Hence, this method provides reliable evidence of the success in the cross-linking process.

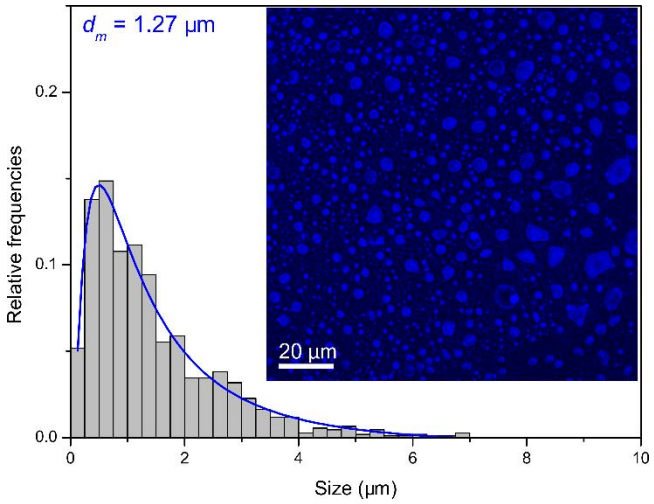

Figure 5. Fluorescence microscopy image of non-cross-linked pyrene-loaded NPs (LMa-1) and the corresponding size distribution obtained from statistical analysis. The curve corresponds to the fit with the log-normal function.

In contrast, a substantial change in size was not observed in stabilized NPs; thus, those loose NPs with the lower cross-link degree (10%, samples LMa-3 and LMa-5) could just slightly augment their size, but not those with a tighter core, such as LMa-2 and LMa-4; due to the absence of fluorescent spots in the images of the latter two samples. Hence, it can be inferred that their particle sizes remained essentially low and stable, and, consequently, out of the range of detection in the fluorescence microscope.

To sum up, it is concluded that the NPs formed are able to effectively incorporate a hydrophobic molecule into their core. Therefore, the study of the inclusion of a drug, pilocarpine, was attempted next.

Loading of pilocarpine

Pilocarpine is a therapeutic molecule with low water solubility and high pharmacological impact; it is clinically used in xerostomy and as an adjunct in the treatment of head and neck cancer; it is also prescribed against Sjogren's Syndrome [40]. The incorporation of the drug into the micelles was followed by UV spectroscopy, using the corresponding non-loaded micelle solution as a blank for each sample. Pilocarpine was promptly loaded into the NPs in the first hours; the drug-NP systems needed between 6 and 24 hours to become stabilized.

In the equilibrated systems, the highest uptake capacities (> 93%) were displayed by cross-linked NPs (from LMb-2 to LMb-5), while sample LMb-1 exhibited the lowest uptake capacity, although the value was still high (89% of the initial pilocarpine).

When both the cross-linker and the degree of cross-linking are set, the porosity and permeability of the core change [9]. These phenomena may also affect the ability to encapsulate and subsequently release therapeutic agents. This is particularly interesting because it offers the possibility of preparing NPs with a core able to control both the drug loading and drug release.

Stimulus-response release of pilocarpine

Linking up a specific stimulus with a mechanism that triggers the drug release is one of the most common approaches to improve therapeutic outcomes. Among the various stimuli, pH changes are considered the most general strategy, aiming at, for example, the extracellular acidic microenvironment and intracellular organelles in solid tumors [41,42].

The pilocarpine-loaded NPs (LMb-1 to LMb-5) behaved as smart systems capable of responding to acidic environments to release the active ingredient when immersed into two

buffered-solutions at pH 7.4 and 3.0. The drug release was studied by UV spectroscopy (**Figure 6**).

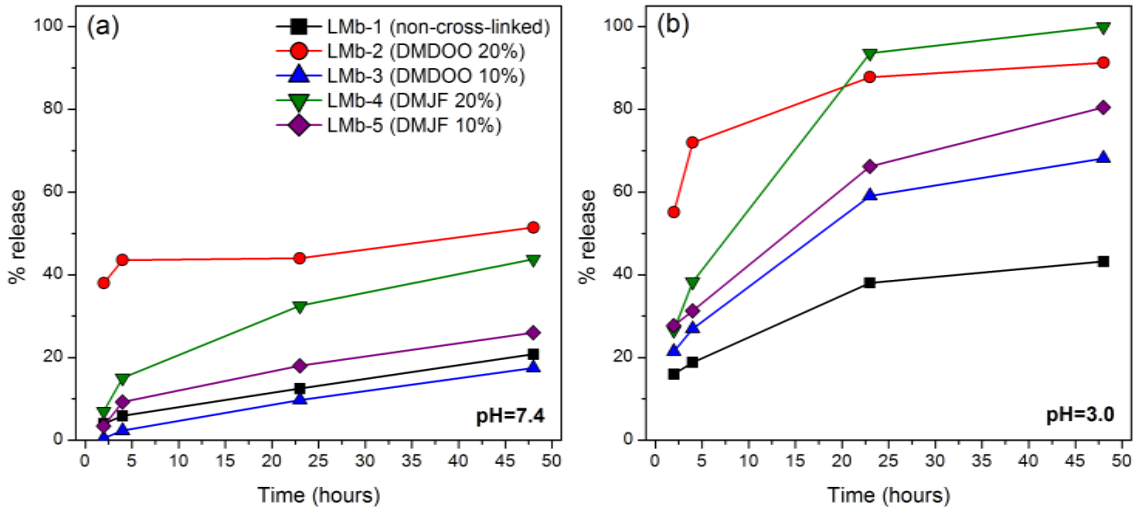

Figure 6. Stimulus-response release of pilocarpine *vs* time (a) at pH 7.4 and (b) at pH 3.0.

Some release was observed at pH 7.4 in all systems (Figure 6a). This could be due to the presence of a significant rate of protonated pilocarpine because of the close value of pK_a of the imidazole ring of pilocarpine (pK_a = 7.0) to the pH of the buffer used.

At pH 3.0, the stabilized NPs showed good stability against dilution, but were prone to release the drug in response to the acidic environment at different rates, depending on the system: the slowest release rates were found in non-cross-linked micelles (Figure 6b). Surprisingly, the degree of cross-linking seems to exert a greater impact on the drug release than the nature of the cross-linker.

4. Conclusions

This work sets out a method to provide stable stimulus-response NPs by total synthesis to achieve the formation of smart drug delivery systems (DDS) useful in biomedicine and pharmacy.

Of the amphiphilic block copolymers synthesized by ATRP, the polymer with best self-assemblable properties in aqueous media was the one with the relative molar composition ($DMA_{31\%}$-$HEMA_{19\%}$)-*block*-($DEA_{45\%}$-$FMA_{5\%}$).

Core cross-linked NPs have been successfully prepared by means of a Diels-Alder coupling reaction between the furan rings in the core and one of the two freshly prepared bisdienophiles, either the hydrophilic or the lipophilic, as cross-linker. The best results were achieved with degrees of cross-linking of 10% and 20%. In all cases the NPs, with size in the range of a few hundred nanometers, remained stable at pH 7.0 and at pH 3.0, as ascertained by means of DLS and SEM studies.

The loading of the model lipophilic molecule, pyrene, was successfully accomplished, and corroborated by fluorescence spectroscopy and fluorescence microscopy. Remarkably, it was verified that the pyrene-loaded non-cross-linked NPs were the only systems able to substantially increase their size (about 10-fold) compared with pyrene-free NPs, supporting the accomplishment of the stabilization achieved in the other systems. The uptake capacity of each dispersion for a therapeutic molecule—pilocarpine—was studied next. The values ranged from 89% to 96% and the drug was promptly loaded into the micelles in the first few hours. Lastly, pilocarpine was released under acidic pH at different rates depending on the system. The degree of cross-linking exerted the greatest impact on the drug release.

Hence, the prepared NPs behaved as smart systems able to control the drug release after acidification of the media. These results bear real relevance to the biomedical field since they are a proof of the concept that the stabilized NPs deploy great potential as controlled drug delivery systems.

Acknowledgements

We thank the Junta de Andalucía (Grant P12-FQM-1553) of Spain for financial support.

References

[1] B. Jeong, A. Gutowska, Lessons from nature: stimuli-responsive polymers and their biomedical applications, Trends Biotechnol. 20 (2002) 305–311. doi:10.1016/S0167-7799(02)01962-5.

[2] C. Ferris, M.V. de Paz, A. Aguilar-de-Leyva, I. Caraballo, J.A. Galbis, Reduction-sensitive functionalized copolyurethanes for biomedical applications., Polym. Chem. 5 (2014) 2370–2381. doi:10.1039/c3py01572f.

[3] X. Ma, H. Tian, Stimuli-responsive supramolecular polymers in aqueous solution, Acc. Chem. Res. 47 (2014) 1971–1981. doi:10.1021/ar500033n.

[4] D. Roy, W.L. Brooks, B.S. Sumerlin, New directions in thermoresponsive polymers, Chem Soc Rev. 42 (2013) 7214–7243. doi:10.1039/c3cs35499g.

[5] M. V de Paz Banez, K.L. Robinson, S.P. Armes, Synthesis and Solution Properties of Dimethylsiloxane-2-(Dimethylamino)ethyl Methacrylate Block Copolymers., Macromolecules. 33 (2000) 451–456. doi:10.1021/ma991665s.

[6] K.L. Robinson, M. V de Paz Banez, X.S. Wang, S.P. Armes, Synthesis of Well-Defined , Semibranched , Hydrophilic - Hydrophobic Block Copolymers Using Atom Transfer Radical Polymerization, Macromolecules. 34 (2001) 5799–5805. doi:10.1021/ma010562i.

[7] E. Galbis, M. V. de Paz, K.L. McGuinness, M. Angulo, C. Valencia, J.A. Galbis, Tandem ATRP/Diels–Alder synthesis of polyHEMA-based hydrogels, Polym. Chem. 5 (2014) 5391–5402. doi:10.1039/C4PY00580E.

[8] E.R. Jones, M. Semsarilar, A. Blanazs, S.P. Armes, Efficient synthesis of amine-functional diblock copolymer nanoparticles via RAFT dispersion polymerization of benzyl methacrylate in alcoholic media, Macromolecules. 45 (2012) 5091–5098. doi:10.1021/ma300898e.

[9] C. Alvarez-Lorenzo, A. Concheiro, Smart drug delivery systems: from fundamentals to the clinic, Chem. Commun. 50 (2014) 7743–7765. doi:10.1039/c4cc01429d.

[10] K. Sapra, A. Sapra, S.K. Singh, S. Kakkar, Self emulsifying drug delivery system: A Tool in Solubility enhancement of Poorly Soluble Drugs, Indo Glob. J. Pharm. Sci. 2 (2012) 313–332.

[11] X.Y. Hu, T. Xiao, C. Lin, F. Huang, L. Wang, Dynamic supramolecular complexes constructed by orthogonal self-assembly, Acc. Chem. Res. 47 (2014) 2041–2051. doi:10.1021/ar5000709.

[12] J. Guo, W. Yang, Y. Deng, C. Wang, S. Fu, Organic-dye-coupled magnetic nanoparticles encaged inside thermoresponsive PNIPAM microcapsules, Small. 1 (2005) 737–741. doi:10.1002/smll.200400145.

[13] M. Kanamala, W.R. Wilson, M. Yang, B.D. Palmer, Z. Wu, Mechanisms and biomaterials in pH-responsive tumour targeted drug delivery: A review, Biomaterials. 85 (2016) 152–167. doi:10.1016/j.biomaterials.2016.01.061.

[14] S.M. Garg, X. Xiong, C. Lu, A. Lavasanifar, Application of Click Chemistry in the Preparation of Poly (ethylene oxide) - block -poly (ε -caprolactone) with Hydrolyzable Cross-Links in the Micellar Core, Macromolecules. 44 (2011) 2058–2066. doi:10.1021/ma102548m.

[15] S. Chen, A.F. Cardozo, C. Julcour, J.F. Blanco, L. Barthe, F. Gayet, M. Lansalot, F. D'Agosto, H. Delmas, E. Manoury, R. Poli, Amphiphilic core-cross-linked micelles functionalized with bis(4-methoxyphenyl)phenylphosphine as catalytic nanoreactors for biphasic hydroformylation, Polymer . 72 (2015) 327–335. doi:10.1016/j.polymer.2015.02.024.

[16] Y. Shi, R.M. Cardoso, C.F. van Nostrum, W.E. Hennink, Anthracene functionalized thermosensitive and UV-crosslinkable polymeric micelles, Polym. Chem. 6 (2015) 2048–2053. doi:10.1039/C4PY01759E.

[17] A. Gandini, The furan/maleimide Diels-Alder reaction: A versatile click-unclick tool in macromolecular synthesis, Prog. Polym. Sci. 38 (2013) 1–29. doi:10.1016/j.progpolymsci.2012.04.002.

[18] A.P. Bapat, J.G. Ray, D. a. Savin, E. a. Hoff, D.L. Patton, B.S. Sumerlin, Dynamic-covalent nanostructures prepared by Diels–Alder reactions of styrene-maleic anhydride-derived copolymers obtained by one-step cascade block copolymerization, Polym. Chem. 3 (2012) 3112. doi:10.1039/c2py20351k.

[19] N.B. Pramanik, N.K. Singha, Amphiphilic functional block copolymers bearing a reactive furfuryl group via RAFT polymerization; reversible core cross-linked micelles via a Diels–Alder "click reaction," RSC Adv. 6 (2016) 2455–2463. doi:10.1039/C5RA22476D.

[20] C.M.Q. Le, H.H.P. Thi, X.T. Cao, G.-D. Kim, C.-W. Oh, K.T. Lim, Redox-responsive core cross-linked micelles of poly(ethylene oxide)- *b* -poly(furfuryl methacrylate) by Diels-Alder reaction for doxorubicin release, J. Polym. Sci. Part A Polym. Chem. 54 (2016) 3741–3750. doi:10.1002/pola.28271.

[21] H.C. Kolb, M.G. Finn, K.B. Sharpless, Click Chemistry: Diverse Chemical Function from a Few Good Reactions, Angew. Chemie Int. Ed. 40 (2001) 2004–2021. doi:10.1002/1521-3773(20010601)40:11<2004::AID-ANIE2004>3.3.CO;2-X.

[22] G. Moad, E. Rizzardo, S.H. Thang, Living Radical Polymerization by the RAFT Process—A First Update, Aust. J. Chem. 59 (2006) 669. doi:10.1071/CH06250.

[23] G. Moad, E. Rizzardo, S.H. Thang, Living radical polymerization by the RAFT process, Aust. J. Chem. 58 (2005) 379–410. doi:10.1071/CH05072.

[24] G. Moad, E. Rizzardo, S.H. Thang, Living radical polymerization by the RAFT process A second update, Aust. J. Chem. 62 (2009) 1402–1472. doi:10.1071/CH09311.

[25] L. Cervera Gontard, D. Ozkaya, R.E. Dunin-Borkowski, A simple algorithm for measuring particle size distributions on an uneven background from TEM images,

Ultramicroscopy. 111 (2011) 101–106. doi:10.1016/j.ultramic.2010.10.011.

[26] C.G.K. De Kruif, T. Huppertz, Casein Micelles: Size distribution in milks from individual cows, J. Agric. Food Chem. 60 (2012) 4649–4655. doi:10.1021/jf301397w.

[27] S. Liu, J.V.M. Weaver, Y. Tang, N.C. Billingham, S.P. Armes, K. Tribe, Synthesis of shell cross-linked micelles with pH-responsive cores using ABC triblock copolymers, Macromolecules. 35 (2002) 6121–6131. doi:10.1021/ma020447n.

[28] J. Zhang, X. Jiang, Y. Zhang, Y. Li, S. Liu, Facile Fabrication of Reversible Core Cross-Linked Micelles Possessing Thermosensitive Swellability., Macromol. (Washington, DC, United States). 40 (2007) 9125–9132. doi:10.1021/ma071564r.

[29] Y. Li, K. Xiao, J. Luo, W. Xiao, J.S. Lee, A.M. Gonik, J. Kato, T.A. Dong, K.S. Lam, Well-defined, reversible disulfide cross-linked micelles for on-demand paclitaxel delivery., Biomaterials. 32 (2011) 6633–6645. doi:10.1016/j.biomaterials.2011.05.050.

[30] H.S. Oberoi, F.C. Laquer, L.A. Marky, A. V Kabanov, T.K. Bronich, Core cross-linked block ionomer micelles as pH-responsive carriers for cis-diamminedichloroplatinum(II)., J. Control. Release. 153 (2011) 64–72. doi:10.1016/j.jconrel.2011.03.028.

[31] K.L. Robinson, M.A. Khan, M. V de Paz Banez, X.S. Wang, S.P. Armes, Controlled Polymerization of 2-Hydroxyethyl Methacrylate by ATRP at Ambient Temperature, Macromolecules. 34 (2001) 3155–3158. doi:10.1021/ma0019611.

[32] V. Bütün, X.-S. Wang, M. V de Paz Banez, K.L. Robinson, N.C. Billingham, S.P. Armes, Z. Tuzar, Synthesis of Shell Cross-Linked Micelles at High Solids in Aqueous Media., Macromolecules. 33 (2000) 1–3. doi:10.1021/ma9914669.

[33] M. V de Paz Banez, K.L. Robinson, M. Vamvakaki, S.F. Lascelles, S.P. Armes, Synthesis of novel cationic polymeric surfactants., Polymer. 41 (2000) 8501–8511. doi:10.1016/S0032-3861(00)00217-2.

[34] L. Piñeiro, M. Novo, W. Al-Soufi, Fluorescence emission of pyrene in surfactant

solutions, Adv. Colloid Interface Sci. 215 (2015) 1–12. doi:10.1016/j.cis.2014.10.010.

[35] M. V de Paz Banez, K.L. Robinson, V. Butun, S.P. Armes, Use of oxyanion-initiated polymerization for the synthesis of amine methacrylate-based homopolymers and block copolymers., Polymer. 42 (2001) 29–37. doi:10.1016/S0032-3861(00)00329-3.

[36] A. Bootz, V. Vogel, D. Schubert, J. Kreuter, Comparison of scanning electron microscopy, dynamic light scattering and analytical ultracentrifugation for the sizing of poly(butyl cyanoacrylate) nanoparticles, Eur. J. Pharm. Biopharm. 57 (2004) 369–375. doi:10.1016/S0939-6411(03)00193-0.

[37] R. Raveendran, G.S. Bhuvaneshwar, C.P. Sharma, In vitro cytotoxicity and cellular uptake of curcumin-loaded Pluronic/Polycaprolactone micelles in colorectal adenocarcinoma cells, J. Biomater. Appl. 27 (2012) 811–827. doi:10.1177/0885328211427473.

[38] G. Bains, A.B. Patel, V. Narayanaswami, Pyrene: A probe to study protein conformation and conformational changes, Molecules. 16 (2011) 7909–7935. doi:10.3390/molecules16097909.

[39] J.A. Ocaña, F.J. Barragán, M. Callejón, Spectrofluorimetric and micelle-enhanced spectrofluorimetric determination of gatifloxacin in human urine and serum, J. Pharm. Biomed. Anal. 37 (2005) 327–332. doi:10.1016/j.jpba.2004.10.027.

[40] A. Mosqueda Taylor, K. Luna Ortiz, M.E. Irigoyen Camacho, M.A. Díaz Franco, A.M. Coll Muñoz, Efecto del clorhidrato de pilocarpina como estimulante de la producción salival en pacientes sometidos a radioterapia de cabeza y cuello, Oral Med. Patol. 9 (2004) 204–211.

[41] M. Kanamala, W.R. Wilson, M. Yang, B.D. Palmer, Z. Wu, Mechanisms and biomaterials in pH-responsive tumour targeted drug delivery: A review, Biomaterials. 85 (2016) 152–167. doi:10.1016/j.biomaterials.2016.01.061.

[42] Y. Shi, C.F. Van Nostrum, W.E. Hennink, Interfacially Hydrazone Cross-linked

Thermosensitive Polymeric Micelles for Acid-Triggered Release of Paclitaxel, ACS Biomater. Sci. Eng. 1 (2015) 393–404. doi:10.1021/acsbiomaterials.5b00006.

List of Captions

Scheme 1. General structure of synthesized methacrylate-based *block*-copolymers and cross-linkers.

Scheme 2. Core cross-linking reaction between DMDOO or DMJF and FMA residues from the micelle core.

Figure 1. SEM micrographs and size distributions extracted from statistical analysis performed on various SEM images for (a) sample M2-1 at pH 7.0 and (b) sample M3-1 at pH 3.0. The curves correspond to the fit of the distributions using a log-normal function.

Figure 2. SEM micrographs of the core cross-linked samples at neutral pH (a) and at acid pH. (b). Size distributions extracted from statistical analysis performed on various SEM images are also plot. The curves correspond to the fit of the distributions using a log-normal function. In the case of sample M2-5, analysis of the size distributions has not been performed because the NPs are strongly agglomerated.

Figure 3. Comparison of the mean NP size determined by DLS and SEM for sample M2 (pH 7.0) and M3 (pH 3.0).

Figure 4. Fluorescence-emission data at 380 nm (arbitrary units) of pyrene loading tests at selected periods of time.

Figure 5. Fluorescence microscopy image of non-cross-linked pyrene-loaded NPs (LMa-1) and the corresponding size distribution obtained from statistical analysis. The curve corresponds to the fit with the log-normal function.

Figure 6. Stimulus-response release of pilocarpine *vs* time (a) at pH 7.4 and (b) at pH 3.0.

Table 1. Values of PdI and average size (D_h, nm) of the NPs prepared at polymer concentrations 0.25 mg/mL, in aqueous media at neutral pH (M2-X) and acid pH (M3-X) and in DMF (M4-X).